
Measurement of volcanic ash in Norwegian air space

WP 1.4.3 Improved estimates of ash cloud top temperature and surface temperature

Arve Kylling



Scientific report

WP 1.4.3: Improved estimates of ash cloud top temperature and surface temperature

Arve Kylling
NILU-Norwegian Institute for Air Research
Kjeller, Norway

September 20, 2013

1 Introduction

For retrieval of ash mass loading from infrared satellite measurements, estimates of the ash cloud temperature and the surface temperature are required. For example, the brightness temperature, T_{11} , in the 10.8 μm band, as observed in the presence of an ash cloud by the Spinning Enhanced Visible and Infrared Imager (SEVIRI), may be written as¹

$$T_{11} = \epsilon_{11}T_c + (1 - \epsilon_{11})T_s. \quad (1)$$

Here ϵ_{11} is the emissivity of the cloud, T_c the brightness temperature of the ash cloud and T_s the brightness temperature of the Earth's surface. The brightness temperature difference, $\Delta T = T_{11} - T_{12}$, between bands centered around 10.8 and 12 μm may be written as (Eq. 5 Prata and Grant, 2001):

$$\Delta T = \Delta T_c(X - X^\beta). \quad (2)$$

where $\Delta T_c = T_s - T_c$, $X = 1 - \Delta_{11}/\Delta T_c$, and $\Delta_{11} = T_s - T_{11}$. Furthermore $\beta = k_{12}/k_{11}$ where k_i is the absorption coefficient. Charts of T_{11} versus ΔT are used to estimate the amount of ash in an ash cloud (Wen and Rose, 1994; Prata and Prata, 2012). Clearly, both quantities depend on the temperature of the ash cloud, T_c , and the surface, T_s . Also, T_c and T_s need to be sufficiently different for an ash cloud to be detectable. Typically one has $T_s > T_c$. Thus, knowledge of both are needed in order to choose the correct T_{11} versus ΔT chart to calculate the ash mass loading from.

Various methods are used to estimate T_c and T_s . Available methods are summarized and compared below.

2 Estimating ash cloud (T_c) and surface (T_s) temperatures

The ash cloud temperature (T_c) and surface temperature (T_s) may be taken from satellite measurements, weather model forecast, or deduced by satellite retrievals.

2.1 Ash cloud (T_c) and surface (T_s) temperatures from SEVIRI measurements

SEVIRI measures the radiance in 12 channels of which 8 are in the thermal infrared. The ash cloud (T_c) and surface (T_s) temperatures may be deduced directly from the window channels (8.7, 10.8 and 12.0 μm) in several ways:

- Within a selected region surrounding the ash cloud the maximum and minimum value of the 12 μm brightness temperature is chosen to represent the surface (T_s) and ash cloud (T_c) brightness temperatures respectively. This method is used for example by Prata and Prata (2012) to initialise the iteration process for determination of ash mass load.
- A similar approach is used in the VOLE ash product from EUMETSAT for determination of ash cloud temperature (T_c)². The VOLE-method is described in de LaaT and van der A De Bilt (2012) from which we quote:

For the estimation of the ash cloud top temperature (T_c), the 3712×3712 pixels image is divided into 128×128 blocks of size 29×29 pixels each.

1. Determine the minimum value of the 12.0 μm channel brightness temperature channel for potentially ash contaminated pixels within each block.
2. Within each block set T_c to the minimum value of 12.0 μm channel in a region of 15×15 blocks centered around the current block.

¹See Appendix A for a justification for Eq. 1 and a derivation of Eq. 2.

²For VOLE information see for example <http://navigator.eumetsat.int/discovery/Start/DirectSearch/DetailResult.do?f%28r0%29=EO:EUM:DAT:MSG:VOLE>

- de LaaT and van der A De Bilt (2012) use a different method for estimation of ash cloud temperature (T_c) and cloud top height. For ash affected pixels the $10.8 \mu\text{m}$ brightness temperature is compared with the local temperature from European Center for Medium range Weather Forecast (ECMWF) analysis data and the height determined accordingly.
- Another approach for the surface temperature (T_s) is to identify clear areas and as a first approach use the channel $10.8 \mu\text{m}$ brightness temperature. Secondly the humidity ($T_{11} - T_{12}$) and the viewing angle may be corrected for (McClain et al., 1985).

2.2 Retrieval of ash cloud temperature (T_c) from SEVIRI measurements

Acknowledging the importance of the ash cloud temperature (T_c) and the difficulty of directly obtaining information from SEVIRI measurements, Francis et al. (2012) and Pavolonis et al. (2013) have devised sophisticated retrieval schemes where the ash cloud temperature (T_c) is estimated simultaneously with ash properties such as mass loading and effective radius. These schemes will be further discussed in Work Package 1.4.5.

2.3 Surface temperature (T_s) from weather forecast models

The surface temperature (T_s) for a given location (pixel) will normally vary slower in time compared to the ash cloud temperature (T_c). Thus, weather forecast model (re)analysis skin-temperature may be used for the surface temperature (T_s) providing such information is available, either from ECMWF or national weather services (met.no).

2.4 Ash cloud temperature (T_c) from lidar measurements

Ash cloud height may be derived from lidar measurements, for example the European Aerosol Research Lidar Network (EARLINET, www.earlinet.org), ceilometers (<http://www.dwd.de/ceilomap>), and Cloud-Aerosol Lidar with Orthogonal Polarization (CALIOP, <http://www-calipso.larc.nasa.gov/>) onboard the Cloud-Aerosol Lidar and Infrared Pathfinder Satellite Observation (CALIPSO) satellite. Lidar observations of ash clouds have also been made from aircraft on campaign basis (Marenco et al. (2011), Schumann et al. (2011) and Chazette et al. (2012)). From the observed ash cloud height the temperature (T_c) of the ash cloud may be estimated by using temperature information from for example weather forecast models. However, the spatial coverage of lidar measurements is limited. Ground-based measurements provide a single point in space. Aircraft measurements are limited by flight restrictions in ash conditions and availability of aircraft. CALIOP provides global coverage, however, with a footprint of 100 m the revisit time is 16 days. It is also noted that ash cloud identification in lidar signals is a non-trivial task. Thus, for ash cloud temperature (T_c) estimates, lidar measurements appear more appropriate and important for validation of other methods.

3 Ash cloud heights during the Eyjafjallajökull 2010 eruption.

The Flexpart Langrangian particle dispersion model (Stohl et al., 2005) ash simulations for the Eyjafjallajökull 2010 eruption (Stohl et al., 2011) have been briefly summarized in the report for work package 1.4.4. The reader is referred to that report for more information including a summary of Flexpart ash cloud altitude results compared with lidar measurements.

The Flexpart ash cloud height is shown in Fig. 1 as a function of distance from the vent and time. The height of the ash cloud is seen to generally decrease as the ash is transported away from the volcano. The initial height of the ash cloud depends on the magnitude of the eruption. The corresponding ash cloud temperature deduced from coupling Flexpart heights and ECMWF reanalysis temperature profiles, is shown in Fig. 2 as a function of distance from the vent and time. As the height of the cloud decreases the temperature generally increases. The ash cloud temperature versus the ash cloud height is shown in Fig. 3. For a given height the temperature may vary with tens of degrees with latitude and longitude. This implies that height information from for example lidars, must be

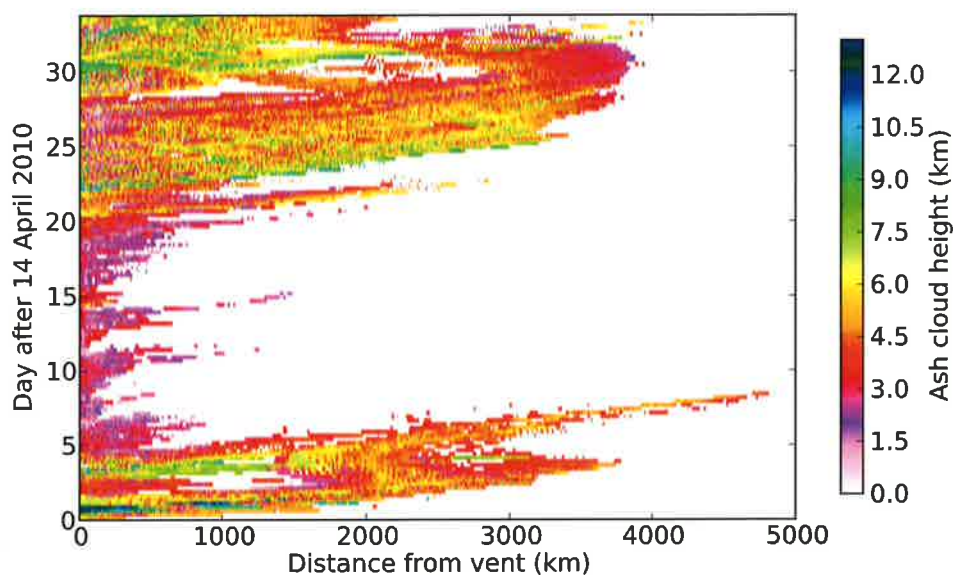


Figure 1: The height of the ash cloud as simulated by Flexpart as a function of distance from the vent and time.

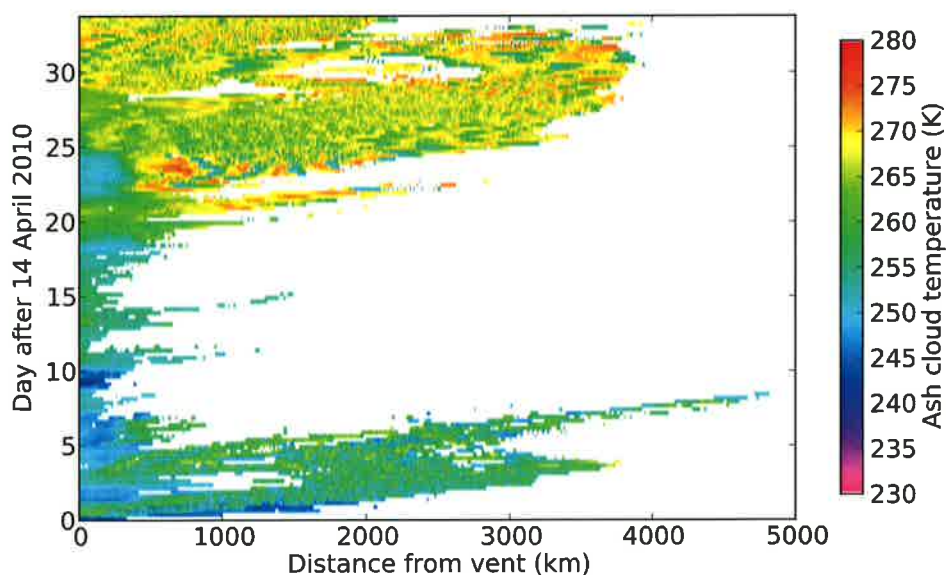


Figure 2: The temperature of the ash cloud as deduced from ECMWF temperature profiles and cloud height from Flexpart, as a function of distance from the vent and time.

coupled with information from other sources to get a representative ash cloud temperature value. Thus, not only height, but also location is important for the best estimate of ash cloud temperature to retrieve an optimal value for the ash mass loading.

One might expect a correspondence between the ash cloud height and the mass loading of the ash cloud. The

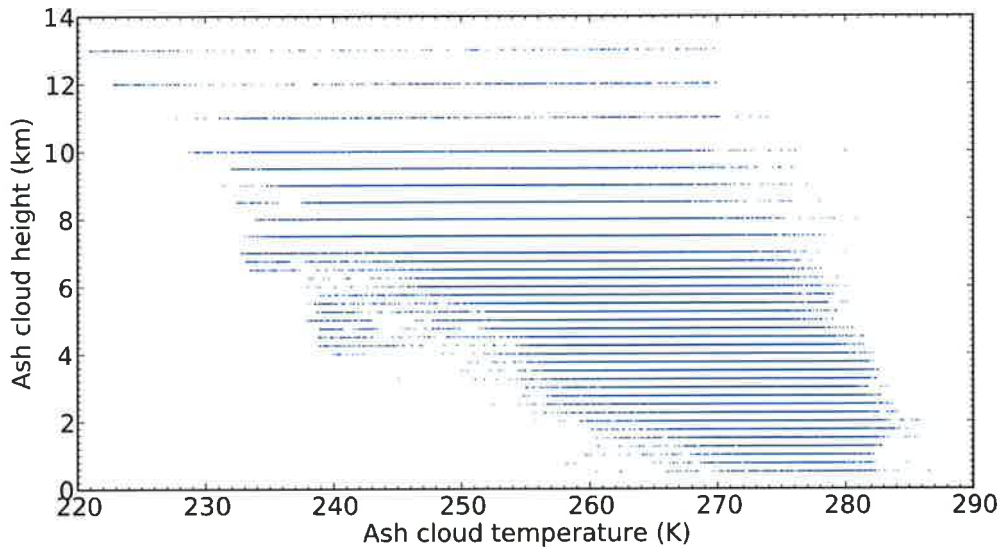


Figure 3: The temperature of the ash cloud as deduced from ECMWF temperature profiles versus cloud height from Flexpart. Note that due to the large number of points, the points merge into horizontal lines for some heights. The vertical stratification is due to the vertical sampling for this Flexpart simulation (250 m).

vertical thickness of the ash cloud is plotted against the logarithm of the mass loading in Fig. 4. For a given ash cloud top height, the spread in the mass loading is large. However, a weak correspondence between the logarithm of the mass loading and the ash cloud height may be identified.

4 The effect of ash cloud height

The effect of ash cloud height on the 10.8 and 12.0 μm brightness temperatures and their difference was investigated by performing radiative transfer simulations with the uvspec radiative transfer model (Mayer and Kylling, 2005). A 1 km layered homogeneous ash cloud was placed at altitudes of 2, 4, 6, 8, 10 and 15 km. For simplicity monodispersed ash particles with radius of 2 μm were used.

The brightness temperature for ash clouds with a large mass loading is largely determined by the ambient temperature at the height of the ash cloud. Thus the atmospheric temperature profile is important. Here the sub-arctic summer atmosphere temperature profile from Anderson et al. (1986) is used. It is shown in Fig. 5 together with the model temperature profile for the tropics. The surface temperature was set to 280 K if not otherwise noted.

In Fig. 6 the 10.8 μm brightness temperature is shown as a function of ash mass loading for ash cloud heights of 15 (black), 10 (purple), 8 (cyan), 6 (red), 4 (green) and 2 km (blue). The corresponding 10.8 and 12.0 μm brightness temperature difference is shown in Fig. 7.

The variations in the brightness temperature and the brightness temperature difference with the ash cloud at different heights are due to the decrease in the ambient temperature with altitude, see Fig. 5. Indeed, the curves for cloud heights of 10 (purple) and 15 km (black) are considerably closer than for the lower heights. This is caused by the ambient temperature being the same at 10 and 15 km, Fig. 5.

The vertical placement of an ash cloud will obviously have a large impact on the retrieved ash mass loading. For example, a 10.8 μm brightness temperature of 260 K will give mass loading of 0.65, 0.9 or 1.5 g/m^2 depending whether the cloud is at 10, 8, or 6 km, Fig. 6.

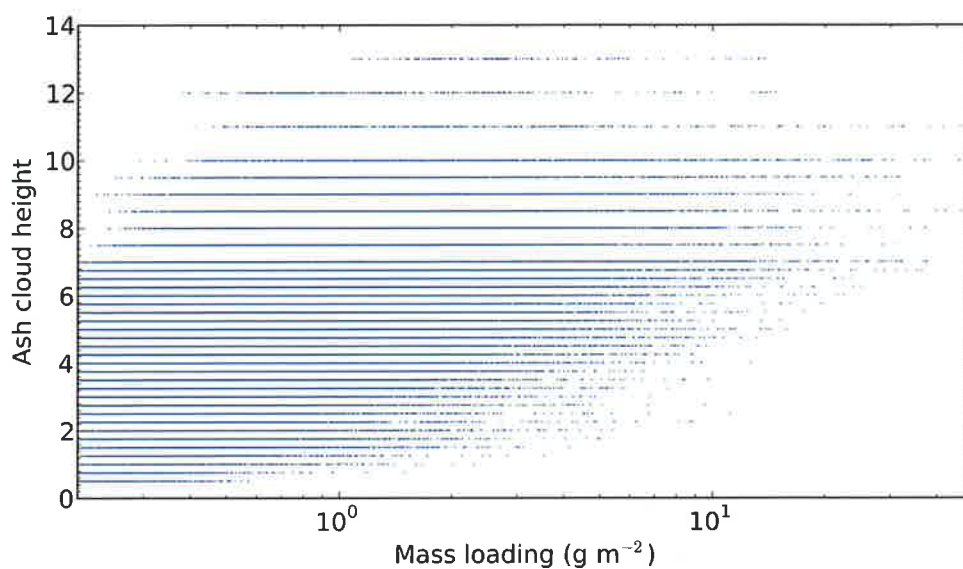


Figure 4: The height of the ash cloud as simulated by Flexpart versus the mass loading. Note logarithmic scale on the x-axis. Also note that due to the large number of points, the points merge into horizontal lines for some heights. The vertical stratification is due to the vertical sampling for this Flexpart simulation (250 m).

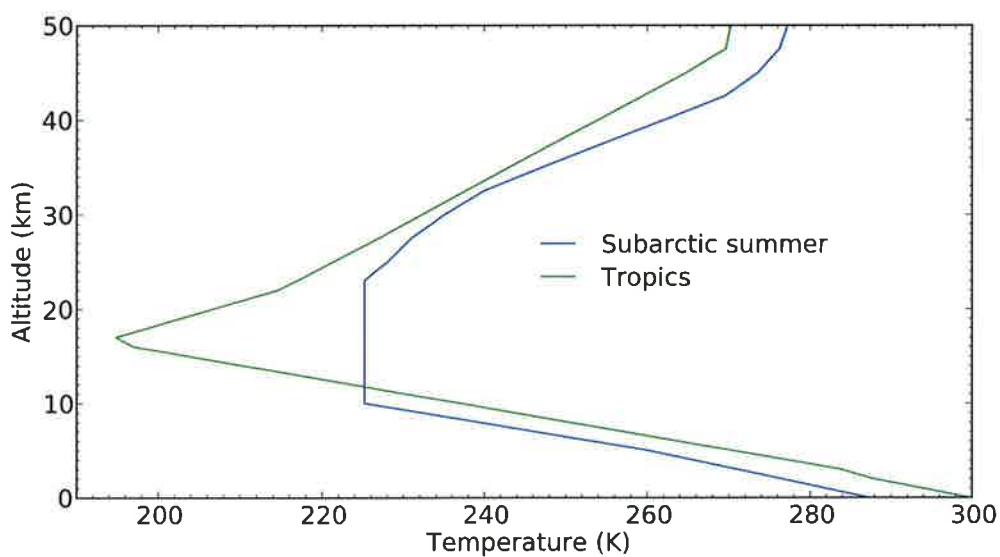


Figure 5: The temperature as a function of altitude for the subarctic summer and tropics atmosphere models of Anderson et al. (1986).

The detection of ash clouds relies on the detection of pixels with a negative 10.8 and 12.0 μm brightness temperature difference. From Fig. 7 it is evident that higher clouds are more readily detected than lower clouds. This

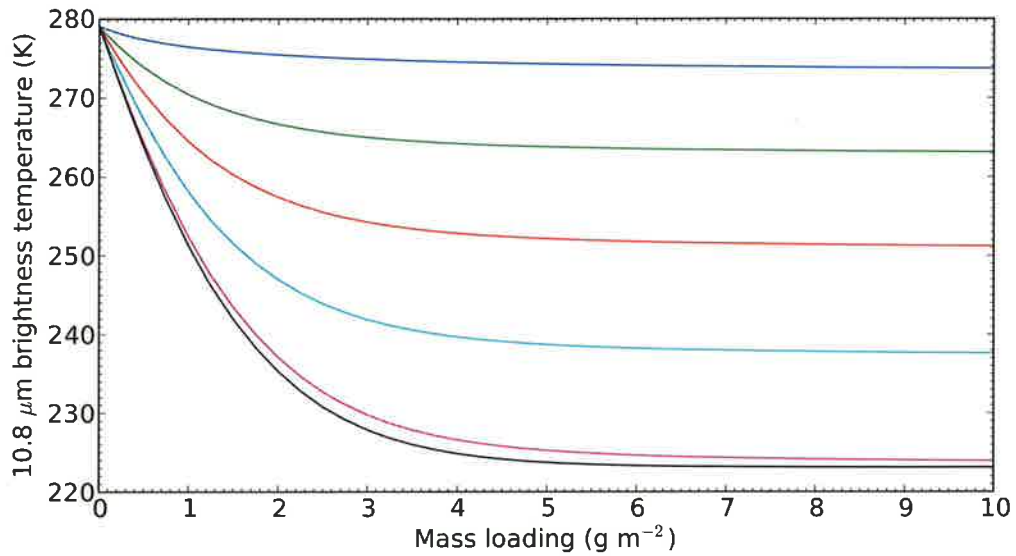


Figure 6: The $10.8 \mu\text{m}$ brightness temperature as a function of ash mass loading for a 1 km thick ash cloud with cloud top height of 15 (black), 10 (purple), 8 (cyan), 6 (red), 4 (green) and 2 km (blue).

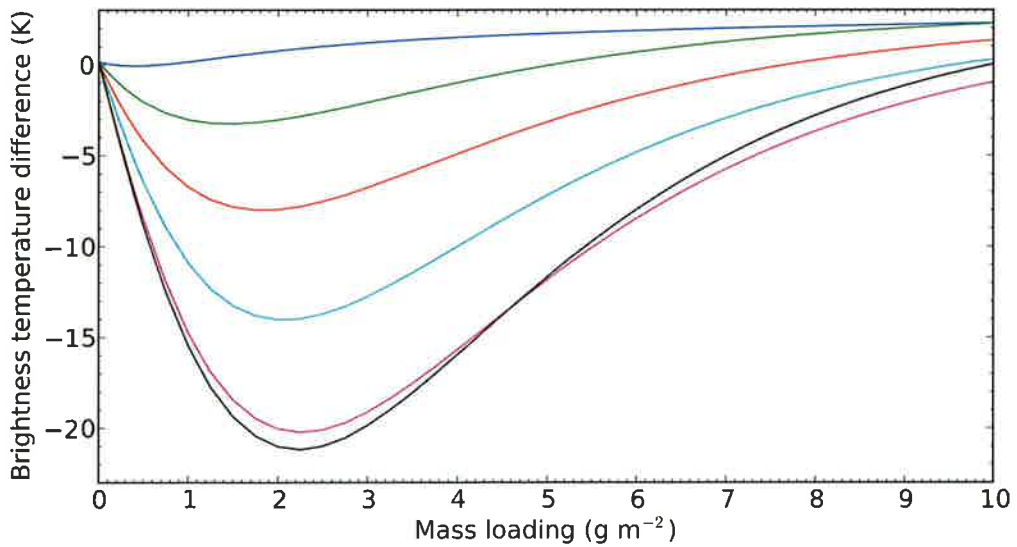


Figure 7: The $10.8\text{-}12.0 \mu\text{m}$ brightness temperature difference as a function of ash mass loading for a 1 km thick ash cloud with cloud top height of 15 (black), 10 (purple), 8 (cyan), 6 (red), 4 (green) and 2 km (blue).

is explained by the increased temperature difference between the cloud and the underlying surface, Eqs. 2 and 8. However, the magnitude of ΔT decreases with increasing mass loading. Thus, thin and thick ash clouds are more challenging to detect by the reverse absorption technique.

5 The effect of surface temperature

For a given location and temperature profile the surface temperature varies less than the atmospheric temperature with altitude. To investigate the effect of surface temperature on the 10.8 and 12.0 μm brightness temperatures and their difference a 1 km thick ash cloud was located at 4 km height which was typical for the Eyjafjallajökull 2010 eruption, see Fig. 1. The surface temperature was set at 280 ± 10 K. The resulting 10.8 μm brightness temperature and the 10.8-12.0 μm brightness temperature difference are shown in Fig. 8. and Fig. 9, respectively.

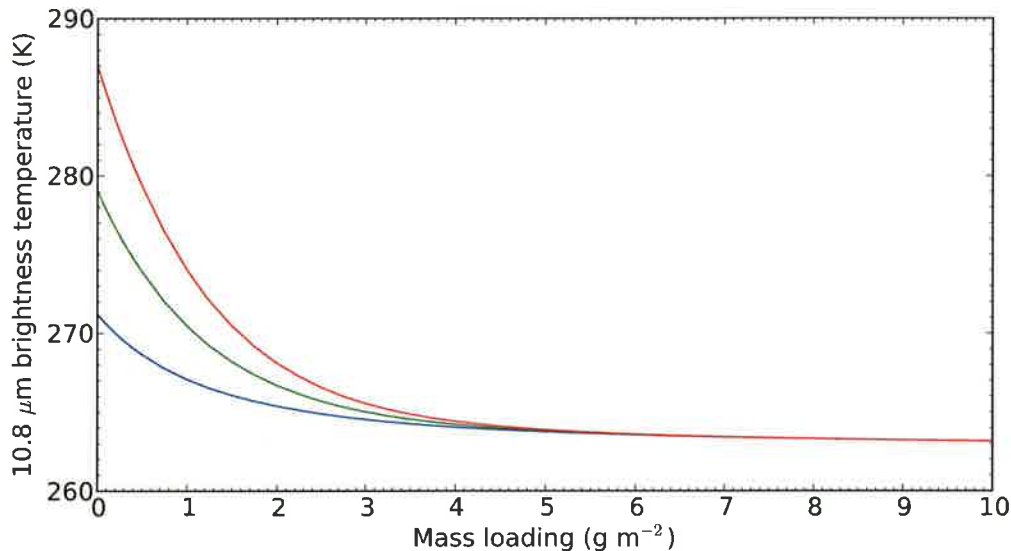


Figure 8: The 10.8 μm brightness temperature as a function of ash mass loading for a 1 km thick ash cloud with cloud top height at 4.0 km and surface temperatures of 270 (blue), 280 (green) and 290 K (red).

As the ash cloud gets thicker, less and less of the infrared radiation emitted by the surface makes it to the top of the atmosphere, and for mass loadings larger than about 4 g/m^2 the 10.8 μm brightness temperature is dominated by the radiation emitted by the cloud, Fig. 8. Thus, for this model ash cloud, the ash mass loading is not sensitive to the surface temperature for mass loadings above 4 g/m^2 . The ash cloud temperature will still be important.

The ash cloud at 4 km has a temperature about 265 K. Thus, increasing the surface temperature from 270 to 290 will increase the 10.8-12.0 μm brightness temperature difference as evident from Fig. 9 and explained by Eqs. 2 and 8. This has also been demonstrated by [Wen and Rose \(1994\)](#) in their Fig. 12. As the brightness temperature difference gets smaller in magnitude, the ash cloud gets harder to detect by the reverse absorption technique.

6 Conclusions

As for ash cloud thickness, report for Work Package 1.4.4, lidars provide the most accurate means for providing an estimate of the ash cloud height. The ash cloud temperature may be deduced from the cloud height by coupling with information from weather forecast models.

The ash cloud from the Eyjafjallajökull 2010 eruption went up to about 12.0 km. Flexpart dispersion model results indicate that the height of the ash cloud decreased with distance from the volcano and that the dependence of height on ash mass loading appears to be weak. Similarly, the ash cloud temperature generally increased with distance from the volcano.

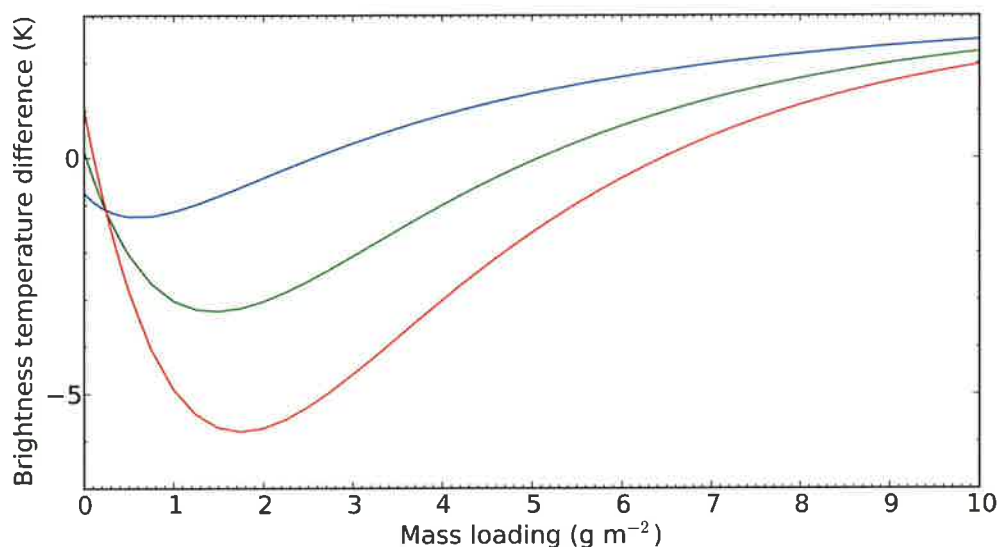


Figure 9: The 10.8-12.0 μm brightness temperature difference as a function of ash mass loading for a 1 km thick ash cloud with cloud top height at 4.0 km and surface temperatures of 270 (blue), 280 (green) and 290 K (red).

Both the 10.8 and 12.0 μm brightness temperatures and their difference varies strongly with the height of the ash cloud. The sensitivity to the surface temperature is largest for moderately thick clouds and disappears for thick clouds.

Various ash cloud detection methods use different surface temperature and ash cloud temperature estimation schemes. These schemes are compared in the report for Work Package 1.4.2.

References

- Anderson, G., Clough, S., Kneizys, F., Chetwynd, J., and Shettle, E.: AFGL atmospheric constituent profiles (0-120 km), Tech. Rep. AFGL-TR-86-0110, Air Force Geophys. Lab., Hanscom Air Force Base, Bedford, Mass., 1986.
- Bohren, C. F. and Clothiaux, E. E.: *Fundamentals of Atmospheric Radiation*, Veimheim, Wiley-VCH, 2006.
- Chazette, P., Dabas, A., Sanak, J., Lardier, M., and Royer, P.: French airborne lidar measurements for Eyjafjallajökull ash plume survey, *Atmos. Chem. Phys.*, 12, 7059–7072, doi:10.5194/acp-12-7059-2012, 2012.
- de LaaT, A. and van der A De Bilt, R.: Validation and evaluation of SEVIRI volcanic ash heights, Tech. rep., KNMI, TR-337, 2012.
- Francis, P. N., Cooke, M. C., and Saunders, R. W.: Retrieval of physical properties of volcanic ash using Meteosat: A case study from the 2010 Eyjafjallajökull eruption, *J. Geophys. Res.*, 117, doi:10.1029/2011JD016788, 2012.
- Marenco, F., Johnson, B., Turnbull, K., Newman, S., Haywood, J., Webster, H., and Ricketts, H.: Airborne lidar observations of the 2010 Eyjafjallajökull volcanic ash plume, *J. Geophys. Res.*, 116, D00U05, doi:10.1029/2011JD016396, 2011.
- Mayer, B. and Kylling, A.: Technical note: the libRadtran software package for radiative transfer calculations-description and examples of use, *Atmos. Chem. Phys.*, 5, 1855–1877, 2005.

- McClain, E. P., Pichel, W. G., and Walton, C. C.: Comparative performance of AVHRR-based multichannel sea surface temperatures, *J. Geophys. Res.*, 90, 11 587–11 601, 1985.
- Pavolonis, M. J., Heidinger, A. K., and Sieglaff, J.: Automated retrievals of volcanic ash and dust cloud properties from upwelling infrared measurements, *J. Geophys. Res.*, 118, 1–23, doi:10.1002/jgrd.50173, 2013.
- Prata, A. J. and Grant, I. F.: Retrieval of microphysical and morphological properties of volcanic ash plumes from satellite data: Application to Mt Ruapehu, New Zealand", *Q. J. R. Meteorol. Soc.*, 127, 2153–2179, 2001.
- Prata, A. J. and Prata, A. T.: Eyjafjallajökull volcanic ash concentrations determined using Spin Enhanced Visible and Infrared Imager measurements, *J. Geophys. Res.*, 117, D00U23, doi:10.1029/2011JD016800, 2012.
- Schumann, U., Weinzierl, B., Reitebuch, O., Schlager, H., Minikin, A., Forster, C., Baumann, R., Sailer, T., Graf, K., Mannstein, H., Vooigt, C., Rahm, S., Simmet, R., Scheibe, M., lichtenstern, M., Stock, P., Rüba, H., Schäuble, D., Tafferger, A., Rautenhaus, M., Gerz, T., Ziereis, H., Krautstrunk, M., Mallaun, C., Gayet, J.-F., Lieke, K., Kandler, K., Ebert, M., Weinbruch, S., Stohl, S., Gasteiger, K., Groß, S., Freudenthaler, V., Wiegner, W., Ansmann, A., Tesche, M., Olafsson, H., and Sturm, K.: Airborne observations of the Eyjafjalla volcano ash cloud over Europe during air space closure in April and May 2010, *Atmos. Chem. Phys.*, 11, doi:10.5194/acp-11-2245-2011, 2011.
- Stohl, A., Forster, C., Frank, A., Seibert, P., and Wotawa, G.: Technical note: The Lagrangian particle dispersion model FLEXPART version 6.2, *Atmos. Chem. Phys.*, 5, 2461–2474, 2005.
- Stohl, A., Prata, A. J., Eckhardt, E., Clarisse, L., Durant, A., Henne, S., Kristiansen, N. I., Minikin, A., Schumann, U., Seibert, P., Stebel, K., Thomas, H. E., Thorsteinsson, T., Tørseth, K., and Weinzierl, B.: Determination of time- and height-resolved volcanic ash emissions and their use for quantitative ash dispersion modeling: the 2010 Eyjafjallajökull eruption, *Atmos. Chem. Phys.*, 11, 4333–4351, 2011.
- Wen, S. and Rose, W. I.: Retrieval of sizes and total masses of particles in volcanic clouds using AVHRR bands 4 and 5, *J. Geophys. Res.*, 99, 5421–5431, 1994.

A Derivation of equation for brightness temperature difference

Infrared (IR) radiation recorded by a satellite instrument viewing the Earth, is emitted from the Earth's surface and the Earth's atmosphere. For an ash cloud at temperature T_c and the Earth's surface at T_s the radiance I_i in wavelength band i , measured by the satellite instrument may be written as:

$$I_i = \epsilon_i B(T_c) + t_i B(T_s). \quad (3)$$

Here ϵ_i is the emissivity of the cloud, t_i the transmissivity of the cloud, and $B(T)$ the Planck function at temperature T . The emissivity and transmissivity are connected via the relationship $\epsilon + r + t = 1$, where r is the reflectivity. Eq. 3 is valid under the assumptions of a plane-parallel and homogeneous cloud, the underlying surface is homogeneous and the ambient atmosphere has no (or little) effect on the radiance. If, furthermore, the underlying surface is assumed to be a blackbody ($r = 0$), Eq. 3 may be written in terms of brightness temperature, T , as (Prata and Grant, 2001):

$$T_i = \epsilon_i T_c + (1 - \epsilon_i) T_s. \quad (4)$$

If multiple scattering is ignored the emissivity may be written as (see for example eq. 2.24 Bohren and Clothiaux (2006))

$$\epsilon_i = 1 - \exp(-k_i L), \quad (5)$$

where L is the geometric thickness of the cloud and k_i is the absorption coefficient.

For SEVIRI observations at bands centered around 11 and 12 μm we get:

$$T_{11} = \epsilon_{11}T_c + (1 - \epsilon_{11})T_s, \quad (6)$$

$$T_{12} = \epsilon_{12}T_c + (1 - \epsilon_{12})T_s. \quad (7)$$

The temperature difference $\Delta T = T_{11} - T_{12}$ thus becomes

$$\Delta T = (\epsilon_{12} - \epsilon_{11})(T_s - T_c). \quad (8)$$

From Eq.5 we have:

$$(1 - \epsilon_{11})^{k_{12}} = (1 - \epsilon_{12})^{k_{11}}, \quad (9)$$

or

$$\epsilon_{12} = 1 - (1 - \epsilon_{11})^\beta \quad (10)$$

where $\beta = k_{12}/k_{11}$. Inserting Eq. 10 in Eq. 8, solving Eq. 6 for ϵ_{11} and inserting in Eq. 8 gives (Eq. 5, Prata and Grant (2001)):

$$\Delta T = \Delta T_c(X - X^\beta). \quad (11)$$

where $\Delta T_c = T_s - T_c$, $X = 1 - \Delta_{11}/\Delta T_c$, and $\Delta_{11} = T_s - T_{11}$.



Norwegian Institute
for Air Research

NILU – Norwegian Institute for Air Research
P.O. Box 100, N-2027 Kjeller, Norway
Associated with CIENS and the Fram Centre
ISO certified according to NS-EN ISO 9001/ISO 14001

REPORT SERIES SCIENTIFIC REPORT	REPORT NO. OR 36/2013	ISBN: 978-82-425-2647-2 (print) 978-82-425-2648-9 (electronic)	
DATE 06/02/2014	SIGN. 	ISSN: 0807-7207	
TITLE Measurement of volcanic ash in Norwegian air space WP 1.4.3 Improved estimates of ash cloud top temperature and surface temperature	PROJECT LEADER Nina I. Kristiansen	NO. OF PAGES 12	PRICE NOK 150.-
	NILU PROJECT NO. O-112109		
AUTHOR(S) Arve Kylling	CLASSIFICATION * A		
	CONTRACT REF.		
QUALITY CONTROLLER: Nina I. Kristiansen			
REPORT PREPARED FOR Ministry of Transport and Communications and AVINOR			
ABSTRACT For retrieval of ash mass loading from infrared satellite measurements, estimates of the ash cloud temperature and the surface temperature are required. The ash cloud temperature and surface temperature may be taken from satellite measurements, weather model forecast, or deduced by satellite retrievals. The report describes various methods to estimate the ash cloud temperature and surface temperature. The impact of varying cloud temperature and surface temperature on the signal measured by an IR-sensor in space is investigated.			
NORWEGIAN TITLE Målinger av vulkanaske i norsk luftrom. WP 1.1.3 Forbedret estimering av askeskytopptemperatur og bakketemperatur			
KEYWORDS Volcanic ash	Remote sensing	Radiative transfer	
ABSTRACT (in Norwegian) Estimering av mengden av aske i en askesky avhenger av askeskyens temperatur og temperaturen til jordens overflate. Askeskytopptemperatur og bakketemperatur kan tas direkte fra satelittmålinger, værvarslingsmodeller eller utledes fra satelittedata. Rapporten beskriver forskjellige metoder for estimering av askeskytopptemperatur og bakketemperatur. Videre diskuteres virkningen av variasjoner i askeskytopptemperatur og bakketemperatur på satelittmålinger av infrarød stråling.			

* Classification
A Unclassified (can be ordered from NILU)
B Restricted distribution
C Classified (not to be distributed)

REFERENCE: O-112109
DATE: JANUARY 2014
ISBN: 978-82-425-2647-2 (print)
978-82-425-2648-9 (electronic)

NILU – Norwegian Institute for Air Research is an independent, nonprofit institution established in 1969. Through its research NILU increases the understanding of climate change, of the composition of the atmosphere, of air quality and of hazardous substances. Based on its research, NILU markets integrated services and products within analyzing, monitoring and consulting. NILU is concerned with increasing public awareness about climate change and environmental pollution.